*Environ. Sci. Technol.* **2009,** *43,* 1952–1961

# Treatment of Nitric Acid-, U(VI)-, and Tc(VII)-Contaminated Groundwater in Intermediate-Scale Physical Models of an In Situ Biobarrier

MANDY M. MICHALSEN,*,† AARON D. PEACOCK,‡ AMANDA N. SMITHGAL,‡ DAVID C. WHITE,‡ ANNE M. SPAIN,§ YAMIL SANCHEZ-ROSARIO,§ LEE R. KRUMHOLZ,§ SHELLY D. KELLY,|| KENNETH M. KEMNER,|| JAMES MCKINLEY,⊥ STEVE M. HEALD,# MARY ANNA BOGLE,▽ DAVID B. WATSON,▽ AND JONATHAN D. ISTOK○

*Environmental Engineering & Technology Section, U.S. Army Corps of Engineers, Seattle, Washington 98134, Center for Biomarker Analysis, University of Tennessee, Knoxville, Tennessee 37932, Department of Botany and Microbiology, University of Oklahoma, Norman, Oklahoma 73019, Biosciences, Argonne National Laboratory, Argonne, Illinois 60439, William R. Wiley Laboratory, Pacific NW National Laboratory, Richland, Washington 99352, Advanced Photon Source, Argonne National Laboratory, Argonne, Illinois 60439, Environmental Sciences Division, Oak Ridge National Laboratory, Oak Ridge, Tennessee 37831, and Department of Civil Engineering, Oregon State University, Corvallis, Oregon 97331*

*Received May 6, 2008. Revised manuscript received December 14, 2008. Accepted December 16, 2008.*

Metal and hydrogen ion acidity and extreme nitrate concentrations at Department of Energy legacy waste sites pose challenges for successful in situ U and Tc bioimmobilization. In this study, we investigated a potential in situ biobarrier configuration designed to neutralize pH and remove nitrate and radionuclides from nitric acid-, U-, and Tc-contaminated groundwater for over 21 months. Ethanol additions to groundwater flowing through native sediment and crushed limestone effectively increased pH (from 4.7 to 6.9), promoted removal of 116 mM nitrate, increased sediment biomass, and immobilized 94% of total U. Increased groundwater pH and significant U removal was also observed in a control column that received no added ethanol. Sequential extraction and XANES analyses showed U in this sediment to be solid-associated U(VI), and EXAFS analysis results were consistent with uranyl orthophosphate $(UO_2)_3(PO_4)_2 \cdot 4H_2O_{(s)}$, which may control U solubility in this system. Ratios of respiratory ubiquinones to menaquinones and copies of dissimilatory nitrite reductase genes, *nirS* and *nirK*, were at least 1 order of magnitude greater in the ethanol-stimulated system compared to the control, indicating that ethanol addition promoted growth of a largely denitrifying microbial community. Sediment 16S rRNA gene clone libraries showed that *Betaproteobacteria* were dominant (89%) near the source of influent acidic groundwater, whereas members of *Gamma-* and *Alphaproteobacteria* and *Bacteroidetes* increased along the flow path as pH increased and nitrate concentrations decreased, indicating spatial shifts in community composition as a function of pH and nitrate concentrations. Results of this study support the utility of biobarriers for treating acidic radionuclide- and nitrate-contaminated groundwater.

## Introduction

The oxidized and mobile forms of U and Tc (such as uranyl carbonates and pertechnetate) have been shown to undergo microbially mediated reductive transformations that decrease their solubility and thus mobility in groundwater in a process referred to as 'bioimmobilization'. Several iron- and sulfate-reducing bacteria are known to reduce soluble U(VI) to insoluble U(IV)-oxides (*1*−*4*) and also Tc(VII) to insoluble Tc(IV)-oxides (*5*−*10*). Although microorganisms with the capability to reduce metals and radionuclides are ubiquitous in the subsurface (*11*), their activity is often limited by the availability of suitable electron donor, high concentrations of competing electron acceptors, or the presence of inhibitory compounds or geochemical conditions. Moreover, other groups of microorganisms and certain chemical processes may reoxidize and thus remobilize U(IV) and Tc(IV), and rates of these competing processes must be controlled so that aqueous U and Tc concentrations remain small (*12*−*15*).

Extreme and variable geochemical conditions typical of Department of Energy (DOE) legacy waste sites pose challenges to successful implementation of in situ bioimmobilization. For example, groundwater at the DOE Field Research Center (FRC) in Oak Ridge, TN, is contaminated with U (up to 210 $\mu$M), Tc (up to 16 nM), extremely high nitrate concentrations (up to 168 mM), and metal and hydrogen ion acidity (*16, 17*). Groundwater geochemistry also varies spatially at this complex site. In the FRC Area 2 field plot, groundwater is pH circumneutral and contains moderate nitrate and aluminum concentrations (0.7 and $1.2 \times 10^{-2}$ mM, respectively), whereas groundwater in the Area 1 field plot (~300 m distance) is acidic and contains extreme levels of dissolved nitrate, aluminum, and calcium (116, 6.78, and 51.1 mM, respectively). Previous studies have shown that several additions of bicarbonate (for pH neutralization) and electron donor (concentrations up to 300 mM) were required to create in situ conditions favorable for U and Tc bioimmobilization at the FRC, and these additions resulted in major shifts in microbial activity, viable biomass, community composition, and physiologic stress responses (*16, 18, 19*). Although some microorganisms can reduce U(VI) under acidic conditions (*20*), successful in situ biostimulation studies conducted at the FRC first neutralized site groundwater ex situ using bicarbonate (*16, 19, 21*).

In situ pH neutralization and removal of extreme nitrate concentrations are significant hurdles that must be overcome for in situ U and Tc bioimmobilization to be feasible at the FRC. In this study we found that ethanol additions to nitric acid-contaminated groundwater flowing through a mixture

* Corresponding author phone: 206 518 2692; fax: 206 764 3706; e-mail: mandy.m.michalsen@usace.army.mil.
† U.S. Army Corps of Engineers.
‡ University of Tennessee.
§ University of Oklahoma.
|| Biosciences, Argonne National Laboratory.
⊥ Pacific NW National Laboratory.
# Advanced Photon Source, Argonne National Laboratory.
▽ Oak Ridge National Laboratory.
○ Oregon State University.


10.1021/es8012485 CCC: $40.75 
Published on Web 02/06/2009

of site sediment and crushed native limestone effectively increased pH, significantly decreased U and other heavy metal concentrations, and sustained nitrate removal for 21 months. Results of our previous study showed that ethanol additions to pH-neutral, low nitrate FRC groundwater effectively stimulated iron and sulfate reduction and sustained U and Tc removal from flowing site groundwater for over 20 months (*22*). Collectively, these results suggest that an in situ biobarrier for U and Tc removal from nitric acid-contaminated FRC groundwater is possible. In addition, microbial community composition data collected over spatially distinct zones of porewater geochemistry indicate that *Betaproteobacteria*, and the genus *Burkholderia* in particular, could be important during ethanol-stimulated nitrate removal from nitric acid-contaminated FRC groundwater.

## Methods

**Biobarrier Model Systems.** The shallow, unconfined aquifer at Oak Ridge National Laboratory is contaminated with nuclear wastes from former unlined storage ponds and was established as a Field Research Center (FRC) by the U.S. DOE (*23*). This study was designed to simulate an in situ biobarrier in FRC Area 1, where groundwater is acidic and sediments forming the shallow (∼7 m) aquifer consist of placed fill underlain by weathered saprolite. Contaminated saprolite from FRC Area 1 (4.7 wt %) and crushed Maynardsville Limestone from nearby outcrops (92 wt %, <0.6 cm sieved) were combined to simulate fill material for a potential biobarrier at the FRC. In an effort to stimulate the denitrifying community and decrease start-up lag time, the contaminated FRC saprolite was incubated with 120 mM nitrate and 100 mM ethanol amended tap water in 1 L glass bottles for 6 to 8 weeks prior to combining with crushed limestone. This "preincubation" could conceivably be performed at a larger scale by incubating site sediment in tanks prior to mixing with limestone for placement during biobarrier construction. Advantages to using this fill material: (1) large quantities of native material were available on site, (2) the crushed limestone created favorable hydraulic conductivity, and (3) the limestone provided buffering capacity to neutralize the acidic groundwater. The fill material was placed to a depth of ∼90 cm in an above-ground rectangular chamber constructed from sheets of 1.3 cm Plexiglas G acrylic (dimensions 226 cm long, 20.3 cm wide, 102 cm deep), which remained open to the atmosphere to allow for gas exchange. Contaminated site groundwater (from well FW21 (*24*)) was pumped through the chamber using a piston pump to simulate groundwater flow through a transect of an in situ biobarrier. This groundwater was aerobic (dissolved oxygen ∼ 6 mg/L), with pH 4.7, and nitrate (116 mM), sulfate (1 mM), U (4.4 $\mu$M), and Tc (12 400 pM) concentrations typical of FRC Area 1 groundwater. Sodium bicarbonate (3.3 wt %) was added to the constructed sediment pack to prevent sorption of U(VI) to sediments, as was previously done in our small-scale laboratory studies (data not shown). Subsequent porewater measurements of total inorganic carbon indicated that the added sodium bicarbonate was flushed from the chamber within four months of operation. The chamber was equipped with an inlet, outlet, 14 sampling ports, manometers, and 8 vertically configured, perforated PVC wells (1.9 cm diameter) positioned along the centerline of the chamber (Supporting Information Figure 1). A syringe pump was used to inject 6 mL of ethanol (190 proof ethyl alcohol) daily into the inlet and into five ethanol injection lines that were attached to wells within the saturated zone, for a target final ethanol concentration of 100 mM. Ethanol has been shown to effectively stimulate U and Tc reduction in low pH environments at the FRC (*16, 19, 21, 25*) and was chosen as an electron donor for its convenience for automated injection and because concentrated ethanol inhibited microbial growth in injection tubing.

An additional above-ground column was constructed using 15.2 cm inside diameter × 245 cm long PVC pipe. This column was packed with the same constructed sediment pack and was operated in an identical fashion as the chamber, only the column was closed to the atmosphere, received no ethanol additions, and served as a control. Both the ethanol-stimulated chamber and control column were deployed and operated in an outdoor tent in Oak Ridge, TN. Pumping rates were selected to yield porewater velocities similar to those reported for site groundwater (0.13−2 m/day *24, 26*). Pumping rates were monitored weekly but varied during the long experiment duration at this remote site; average flow rates were 3.5 ± 2.7 mL/min in the chamber and 2.1 ± 0.70 in the control. Porewater samples were collected from all sampling ports located along the length of chamber on a weekly basis and from the control on a monthly basis; changes in flow rates and manometer levels were monitored with each sampling. Quantities of analytes removed during the experiment were quantified by integrating flow rates and differences in inlet and outlet concentrations. Average daily temperatures in Oak Ridge, TN, during the experiment were collected from the data archive maintained by the National Weather Service Forecast Office (available online http://www.srh.noaa.gov/mrx/oqt/clioqt.php). See Supporting Information Figure 2 for a detailed experimental timeline.

**Data Analysis.** Tracer tests (chamber only) were conducted by amending influent groundwater with 1.25 mM bromide and sampling to obtain breakthrough curves. Porewater velocities were determined by fitting bromide breakthrough concentrations to the advection dispersion equation using CXTFIT (*27*). Porewater velocities were used to calculate travel times from the inlet to each sampling port. Apparent zero-order removal rates for nitrate, U, and Tc were computed by performing a least-squares regression of concentration profiles and travel times. Porewater mass balance calculations were performed by integrating measured pumping rates and differences in inlet and outlet concentrations. Contaminant removal efficiency values were calculated as the total mass of contaminant removed (from the mass balance) divided by the total volume of groundwater that passed through the system. Hydraulic conductivity was computed using measured pumping rates and hydraulic heads.

**Sediment Uranium Analysis.** It was only possible to collect a single sediment sample for this special analysis because of instrument availability and project budget. A single sediment sample was collected from the saturated zone near the chamber inlet and was sequentially extracted to quantify U using previously published methods (*28, 29*). Briefly, the sediment sample was extracted sequentially with anoxic deionized (DI) water, anoxic, 1 M bicarbonate, and finally nitric acid. Using previously published criteria (*28, 29*), uranium extracted with deionized (DI) water and bicarbonate was assumed to be U(VI), and acid-extractable uranium was assumed to be U(IV). U X-ray absorption measurements (XANES and EXAFS) were collected at PNC-CAT and MR-CAT (*30*) at the APS. The speciation of U in this sediment sample was determined by modeling the extended X-ray absorption fine structure portion of the spectrum. See Supporting Information for additional detailed methods.

**Sediment Collection and Lipid Analyses.** Sediment samples were collected for microbial community characterization from six locations within the chamber saturated zone after 16 months of operation and from the eight sampling ports along the control after 9.8 months of operation (Supporting Information Figure 3). Chamber sediment core locations and corresponding characteristic porewater concentrations at these locations are summarized in Table 1.

**TABLE 1. Sediment Core Locations within the Ethanol Stimulated Chamber and Corresponding Porewater Chemistry**

| | distance to core location from inlet, cm | depth to core sample from surface of fill, cm | characteristic porewater concentrations | | | | |
|---|---|---|---|---|---|---|---|
| | | | U, $\mu$M | Tc, pM | $NO_3$, mM | $NO_2$, mM | pH |
| core 1 | 2.81 | 21.0 | 4.4 | 12408 | 116 | 0.03 | 4.7 |
| core 2 | 41.9 | 24.0 | 0.31 | 10889 | 106 | 5.0 | 6.9 |
| core 3 | 104 | 22.9 | 0.29 | 8854 | 85.4 | 8.5 | 7.3 |
| core 4 | 137 | 24.0 | 0.16 | 7763 | 66.5 | 9.1 | 7.4 |
| core 5 | 168 | 24.8 | 0.17 | 6057 | 55.3 | 9.7 | 7.6 |
| core 6 | 193 | 28.6 | 0.14 | 6589 | 67.4 | 8.8 | 7.6 |

Total lipids were extracted from the sediment samples using a modified Blyer and Dyer method (*31, 32*). Silicic acid chromatography was used to separate the total lipids into polar, neutral, and glycolipid fractions (*33*). The polar lipid fraction was subsequently transesterified using mild alkaline methanolysis to form fatty acid methyl esters (FAMEs) (ref *33* with modifications in ref *34*). The different lipid fractions were quantified as previously described (*35*).

**Molecular Microbial Community Analyses.** DNA was extracted from all chamber and control sediment samples using the FastDNA spin kit for soil (BIO101, La Jolla, CA) and eluted in 100 $\mu$L of 1/10 TE buffer. Quantitative PCR (Q-PCR) was performed by Microbial Insights Inc. (Rockford, TN) as described previously (*35*) to target and quantify different groups of bacteria. TaqMan-based PCR was used to detect the following groups using the indicated probes and forward/reverse primers: Bacteria (TM1389, BACT1369/PROK1492R (*36*)); *Deltaproteobacteria* (GBC2, 361F/685R (*37*)); *Geobacteraceae* (GBC2, 561F/825R (*37*)). SYBR green PCR was used to detect the following targets using the indicated forward/reverse primers: *nirS* gene (1260F/1363R (*38*)) and *nirK* gene (nirK876F/nirK1040R (*39*)). DGGE analysis was performed on PCR-amplified partial 16S rRNA genes from the chamber sediment cores only using the 16S rRNA primer set 341F/519R with a 40-bp GC clamp on the forward primer (*40*). 16S rRNA gene clone libraries were constructed from the three sediment core samples nearest to the chamber inlet only. PCR products from the sediment-extracted DNA were obtained using primers uni8F/EUB805R and purified using the Geneclean Turbo Kit Bio 101. Details of our Q-PCR, DGGE, and 16S rRNA gene clone library analysis methods were previously described (*35*). GenBank accession numbers for sequences from this study are EF422267 to EF422276 and EF507905 to EF507962 for DGGE gel band sequences and clone sequences, respectively.

**Analytical Methods.** pH was measured by a glass electrode and meter. Inorganic anion (nitrate, nitrite, sulfate, chloride, bromide) concentrations were measured by ion chromatography. Ethanol was measured by gas chromatography with flame ionization detection. Uranium concentrations were measured using a kinetic phosphorescence analyzer (KPA-11, CHEMcheck Instruments). Technetium was measured using a liquid scintillation analyzer (Tri-Carb 2900TR, Packard Instruments). See Supporting Information for additional detailed methods.

## Results

**Biobarrier Model Performance.** Differences between the ethanol-amended chamber and control are summarized in Figure 1, which shows the long-term average porewater concentrations and pH values over the entire experiment for both systems. During the 21 months of chamber operation, 2184 L of groundwater was passed through the chamber, pH was increased on average from 4.7 to 7.6, and 340 mol of ethanol, 6.8 $\mu$mol of Tc, 8.3 mmol of U, and 87 mol of nitrate were removed from influent groundwater, and 11 mol of nitrite produced during denitrification were detected in the chamber effluent. During the 15.7 months of control operation, 1366 L of groundwater was passed through the control, pH was increased on average from 4.2 to 6.3, and 3.7 $\mu$mol of Tc, 3.4 mmol of U, and 3.6 mol of nitrate were removed from influent groundwater, and 41.5 mmol of nitrite produced during denitrification were detected in control effluent. On the basis of the mass balance performed on the routinely measured analytes shown in Figure 1, 93% less nitrate, 35% less U, and 13% less Tc was removed per liter of groundwater in the control compared to the chamber.

U concentrations decreased with increased pH in the chamber and control (Figure 1). Sediment near the chamber inlet where pH neutralization occurred contained 14 ppb total extractable U ($5.88 \times 10^{-2}$ $\mu$mol per gram dry sediment). One third of the total U was extracted using 1 M bicarbonate and was considered sorbed U(VI), while the remaining U was extracted using nitric acid and was considered U(IV) (*28, 29*). It is unlikely that U(IV) was present in significant quantities in the chamber sediment near the inlet where U deposition occurred, given the continuous high nitrate concentration in this location. Indeed, XANES spectra collected from this sediment showed 100% of the U in this sample to be U(VI), suggesting the majority of U was recalcitrant U(VI) that was not effectively extracted by the 1 M bicarbonate solution. The distribution of Ca and U in core 1 sediments shows elevated U concentrations on the outer regions of the limestone particles (Figure 2A), which is consistent with the precipitation of U(VI) on the limestone

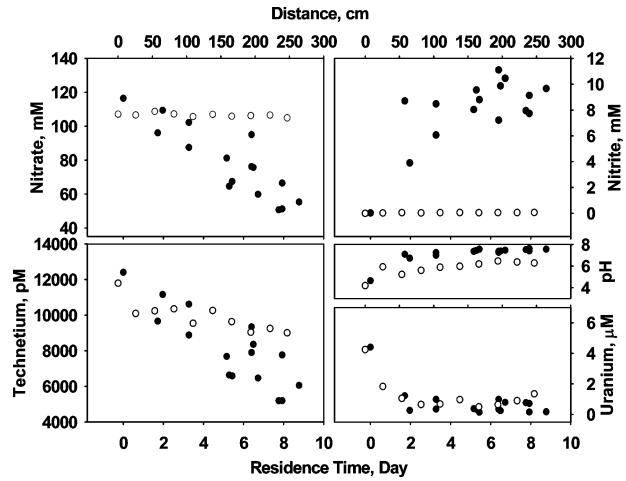


**FIGURE 1. Average concentration profiles in the ethanol stimulated chamber verses travel time over 21 months (solid symbols, $n$ = 130), where inlet concentrations correspond to time zero. Average control concentrations over 18 months (open symbols, $n$ = 16) are shown verses distance along the column flow path because no tracer tests were conducted in the control and travel times were unknown.**

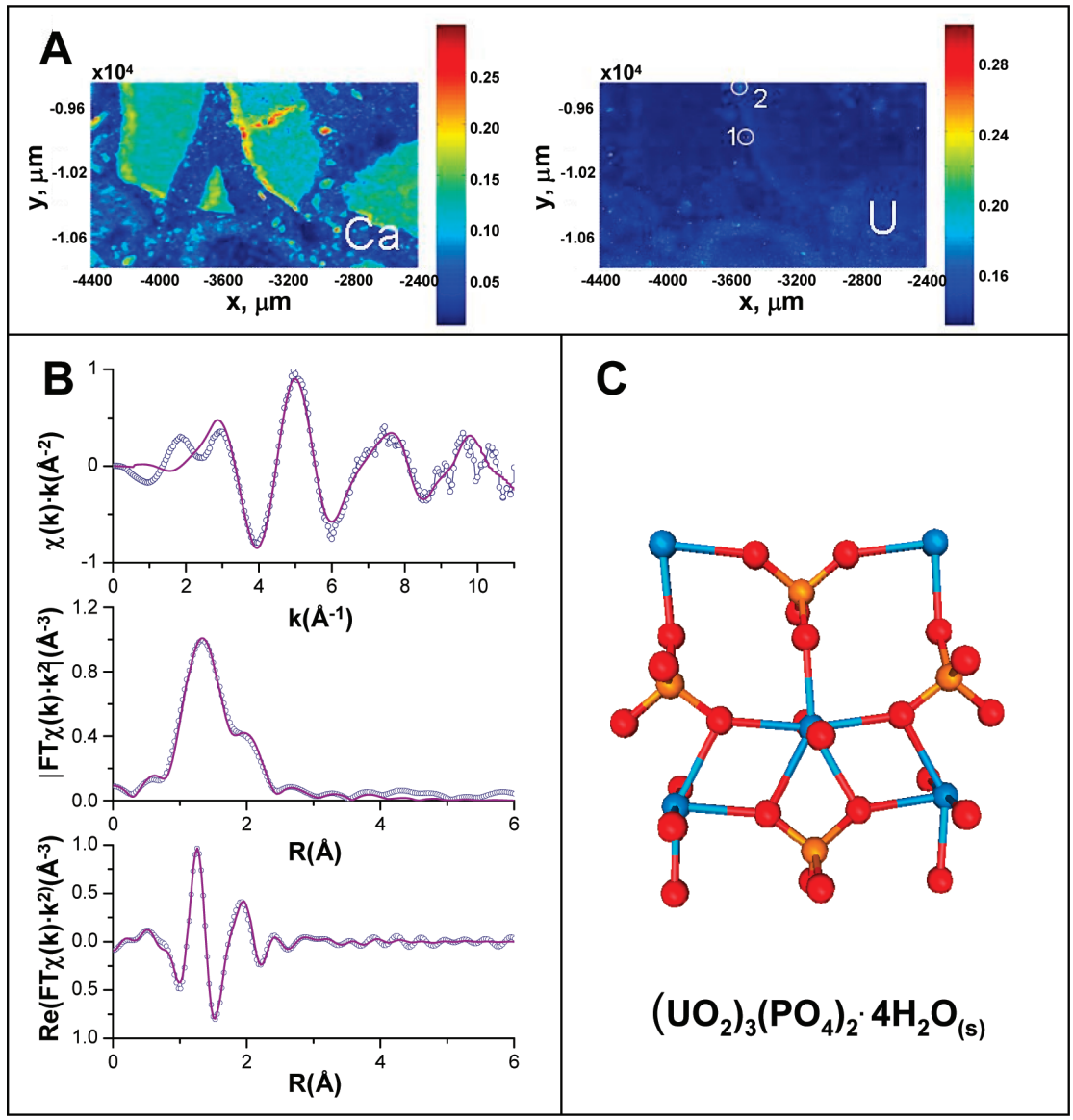


**FIGURE 2. X-ray analysis of chamber core 1 sediment. (A) X-ray fluorescence of sediment showing the distribution of Ca (left) and U (right). Regions 1 and 2 (circled) were further probed for XANES and EXAFS measurements. (B) EXAFS spectra collected from region 2 (open symbols) and model fit based on the structure of uranyl orthophosphate $(UO_2)_3(PO_4)_2 \cdot 4H_2O_{(s)}$. Top: EXAFS $\chi(k)$ spectrum, middle: magnitude of Fourier transform of EXAFS spectrum, bottom: real part of Fourier transform of EXAFS spectrum. (C) Structural model of uranyl orthophosphate. Blue, red, and orange spheres represent U, O, and P atoms, respectively.**

surface. The EXAFS spectra collected from this sediment is consistent with the structure of $(UO_2)_3(PO_4)_2 \cdot 4H_2O_{(s)}$ (Figure 2B and 2C), which to our knowledge has not been previously detected in natural samples (*41*) but could be important in controlling U solubility in this system. Although phosphate concentrations were not measured in this study, historical data for groundwater from well FW21 (source well for this study, data available online (*24*)) indicate a total phosphorus concentration of 4.73 mg/L.

U removal rates remained fairly constant (2.49 ± 1.63 $\mu$M/day), whereas nitrate and Tc removal rates fluctuated during this long-term outdoor experiment (Figure 3). Nitrate and Tc removal rates increased to a maximum of 23 mM day$^{-1}$ and 1897 pM day$^{-1}$, respectively, early during the experiment. While nitrate and Tc concentrations decreased concomitantly and to similar extents in the chamber (55% on average, Figure 3), nitrate concentrations decreased only slightly and Tc concentrations were decreased by 35% on average in the control. We did not monitor Fe(II) in chamber porewater based on results of laboratory-scale chamber experiments conducted with pH-neutralized FRC Area 1 groundwater, which indicated that nitrate reduction would predominate in the chamber and prevent the onset of Fe(III) reduction (data not shown). However, it was not possible to exclude a role for Fe(II) in the observed Tc removal because Fe(II) concentrations were not monitored. In a follow-up laboratory batch experiment, ethanol addition to a mixture of high-nitrate artificial groundwater, FRC sediment, and Maynardsville limestone resulted in a 20% reduction in aqueous Tc concentrations under denitrifying conditions; Fe(II) concentrations did not exceed 2.95 $\mu$M (see Supporting Information Figure 4 and associated text).

Average ethanol concentrations decreased initially due to microbial consumption. In order to ensure adequate electron donor in the chamber, influent site groundwater was amended with 95 mM ethanol beginning on day 179 to supplement daily injections. Hydraulic conductivity increased in the chamber when rates of nitrate removal were small but subsequently decreased when rates of nitrate removal increased, suggesting a link between increased production of nitrogen gas or biomass during denitrification and decreased hydraulic conductivity. Hydraulic conductivity in

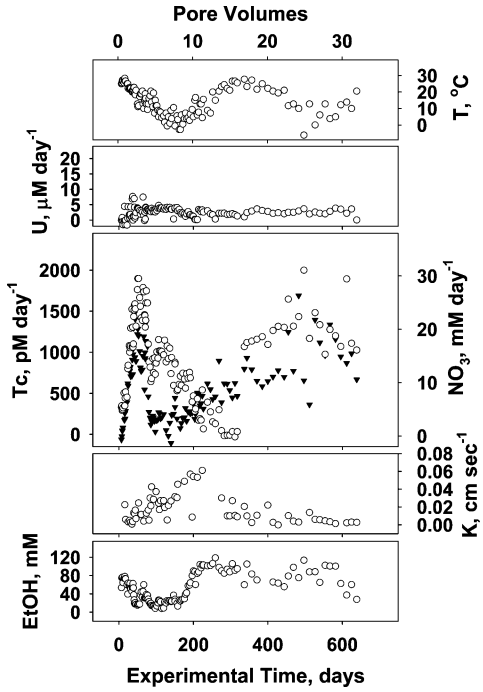


**FIGURE 3. Apparent zero-order rates of U, Tc, and nitrate removal, as well as average daily temperatures, porewater ethanol concentrations, and hydraulic conductivity (K) verses experimental time (lower *x*-axis) and total pore volumes passed through the chamber (upper *x*-axis). Filled triangles represent nitrate removal rates and open circles represent all other data.**

the chamber averaged $1.93 \times 10^{-4}$ m $s^{-1}$ initially but decreased to an average of $2.85 \times 10^{-5}$ m $s^{-1}$ by the end of the experiment.

**Microbial Community Composition.** *Phospholipid Fatty Acid (PLFA) Results.* PLFA biomass was 65% greater on average in the chamber compared to the control, confirming that ethanol additions promoted microbial growth. Differences in percentages of total PLFA within PLFA groups were observed as well (Table 2). Percentages of midchain branched saturates, indicators of sulfate reducing bacteria (*42, 43*), were smaller on average in the chamber compared to the control. Hydroxy fatty acids, which are common though not exclusive to Gram-negative bacteria (*44, 45*), were greater on average in the chamber compared to the control. Differences in percentages of the remaining PLFA groups were not observed.

Elevated ratios of both cyclopropyl fatty acids to their monoenoic precursors and ratios of monounsaturated trans to cis isomers have been linked with starvation, stationary-phase growth, nutrient deprivation (*33, 46*−*49*), and also ethanol exposure (≥1% by volume) (*49*). Both of these ratios were increased in the chamber compared to the control (Table 2), suggesting a community response to high ethanol concentrations (120 mM, 0.7% by volume), limited microbial growth when sediment samples were collected, or nutrient limitations occurring as high levels of carbon but no other nutrients are added. Elevated ratios of iso- to anteiso-saturated fatty acids have been linked with bacterial membrane fluidity changes in response to environmental stress, particularly temperature (*50*−*52*). Though both models were subject to the same outdoor temperature shifts during the experiment, the ratio of iso- to anteiso-saturated fatty acids was decreased in the chamber compared to the control, suggesting less environmental stress in the chamber compared to the control. Respiratory ubiquinones are associated with high energy electron acceptors such as oxygen and nitrate while menaquinones are associated with other types of anaerobic respiration (*53*); thus, elevated ratios of ubiquinones to menaquinones (UQ/MQ) as observed in the chamber (a 6 fold increase) confirm a shift toward a denitrifying community.

*Quantitative-PCR Results.* Bacterial 16S rRNA gene copy numbers were more than 2 orders of magnitude greater in the chamber compared to the control, further substantiating that ethanol additions promoted microbial growth (Table 2). Dissimilatory nitrite reductase genes, *nirS* and *nirK*, were both 2 orders of magnitude greater in the chamber compared to the control. *Geobacteraceae* were detected in several chamber samples but were not detectable in control samples using our methods. *Deltaproteobacteria* were not significantly different on average in the chamber compared to the control.

*Community Composition of Chamber Core Sediment.* No visually dominant bands were detected in the chamber core 1 sediment sample DGGE profile (Supporting Information Figure 5). Selected DGGE band sequences from subsequent chamber core sediment samples were most similar to the genera *Pseudomonas* (Core 2-A, Core 2-B, Core 5-F, Core 5-G, Core 6-J), *Sporomusa* (Core 5-H), *Castellaniella* (Core 2-C, Core 5-I), and *Bacteroides* (Core 4-E, Core 3-D) (Supporting Information Figure 6). Most sequences detected in chamber core 1 and 2 sediment 16S rRNA gene libraries (100 and 89%, respectively) belonged to the Proteobacteria phylum (Table 3). In chamber core 1 sediments, 86% of sequences belonged to *Betaproteobacteria*; other sequences detected belonged to *Alpha-* (8%) and *Gammaproteobacteria* (6%). *Betaproteobacteria* sequences were also dominant in core 2 sediment (64%); other sequences detected belonged to *Gamma-* (21%) and *Alphaproteobacteria* (4%), *Acidobacteria* (4%), *Bacteriodetes* (3%), *Firmicutes* (3%), and *Actinobacteria* (1%). In contrast to core 1 and 2 sediments, *Bacteroidetes* (29%) and *Alphaproteobacteria* (27%) sequences were dominant in chamber core 3 sediments, and *Betaproteobacteria* sequences were detected in smaller proportions (13%). Other sequences detected in core 3 sediments were *Actinobacteria* (13%), *Firmicutes* (9%), *Gammaproteobacteria* (5%), and *Acidobacteria* (4%).

The majority of clone sequences within the chamber core 1 and 2 sediment 16S rRNA gene clone libraries (59% and 41%, respectively) shared close homology with *Burkholderia fungorum* within the *Betaproteobacteria* (Supporting Information Figure 6). Other clone sequences detected in core 1 sediment shared close homology with *Variovorax paradoxus*, which was also previously detected in pH 5.5, low nitrate FRC groundwater (*54*). Other clone sequences detected in core 1 shared close homology with *Ralstonia insidiosa*; *Ralstonia* sequences were also dominant (86%) in RNA-based clone libraries from acidic FRC sediments (*55*). Also within the *Betaproteobacteria*, DGGE band sequences (Core 5-I, Core 2-C) and other clone sequences from this study shared close homology with *Castellaniella defragrans* and several other clones and isolates from acidic FRC sediments (*19, 21*). Other *Betaproteobacteria* clone sequences were similar to *Acidovorax defluvii*. Interestingly, an *Acidovorax* isolate from a denitrifying fluidized-bed reactor used to treat FRC groundwater was also implicated in U(VI) reduction (*56*). *Betaproteobacteria* clones were also detected in significant proportions in ethanol- and nitrate-amended FRC Area 2 sediment microcosms (*57*). Within the *Gammaproteobacteria*, DGGE band sequences (Core 2-B, Core 5-G, Core 6-J) and clone sequences from this study shared close homology with *Pseudomonas stuzeri*; other DGGE band sequences (Core 2-A, Core 5-F) were also similar to other *Pseudomonas* species. Other *Gammaproteobacteria* clone sequences from this study shared close homology with a *Rhodanobacter* clone previously detected in U contaminated FRC sediment (*58*). Within the *Firmicutes* phylum, DGGE band sequence Core 5-H was most similar to the obligate anaerobe *Sporomusa silvacetica* (*59*),

**TABLE 2. Data Summary of Q-PCR and PLFA Groups for Chamber Core (left, $n = 6$) and Control Sediment Samples (right, $n = 8$)[a]**

| | chamber core sediment samples | | control sediment samples | |
|---|---|---|---|---|
| | avg | stdev | avg | stdev |
| PLFA | | | | |
| viable biomass, cells/gram sediment | $2.83 \times 10^8$ | $1.42 \times 10^8$ | $9.85 \times 10^7$ | $5.62 \times 10^7$ |
| community structure (% total PLFA) | | | | |
| midchain branched saturates | 1.36 | 0.23 | 4.3 | 0.90 |
| hydroxy | 0.61 | 0.52 | 0.00 | 0.00 |
| terminally branched saturates | 12.4 | 2.63 | 10.8 | 1.68 |
| branched monounsaturates | 2.81 | 0.47 | 2.51 | 0.37 |
| monounsaturates | 54.0 | 2.06 | 55.0 | 1.73 |
| normal saturates | 28.0 | 2.10 | 26.9 | 2.48 |
| polyunsaturates | 0.79 | 1.22 | 0.46 | 0.23 |
| metabolic status (ratio) | | | | |
| cy17:0/16:1w7c | 2.36 | 0.710 | 1.23 | 0.483 |
| cy19:0/18:17c | 1.518 | 0.327 | 0.78 | 0.225 |
| total cyc/cis | 3.88 | 1.02 | 2.01 | 0.704 |
| 16:1w7t/16:1w7c | 0.314 | 0.102 | 0.084 | 0.007 |
| 18:1w7t/18:1w7c | 0.097 | 0.049 | 0.069 | 0.008 |
| total trans/cis | 0.411 | 0.141 | 0.153 | 0.012 |
| i15:0/a15:0 | 0.605 | 0.168 | 1.06 | 0.074 |
| i17:0/a17:0 | 0.640 | 0.189 | 1.09 | 0.179 |
| total iso/anteiso | 1.24 | 0.270 | 2.15 | 0.217 |
| ubiquinones/menaquinones (ratio) | 22.1 | 4.12 | 3.63 | 1.86 |
| Q-PCR, Copies/Gram Sediment | | | | |
| Eubacterial 16S rRNA | $1.60 \times 10^9$ | $8.48 \times 10^8$ | $7.06 \times 10^6$ | $3.18 \times 10^6$ |
| *nirS* | $7.56 \times 10^8$ | $3.89 \times 10^8$ | $2.12 \times 10^6$ | $1.40 \times 10^6$ |
| *nirK* | $2.01 \times 10^8$ | $1.03 \times 10^8$ | $1.15 \times 10^6$ | $1.49 \times 10^6$ |
| $\delta$-Proteobacteria[b] | $3.22 \times 10^4$ | $4.34 \times 10^4$ | $5.66 \times 10^2$ | $1.27 \times 10^3$ |
| *Geobacteraceae* | <100[c] | – | ND[d] | – |

[a] Individual data values for all chamber core and control sediment samples are included in Supporting Information. [b] The full detection limit of 100 was utilized to obtain the average and standard deviation values. [c] <100 indicates below detection limit, ND or estimated value in all samples. [d] ND, not detected in any sample.

**TABLE 3. Distribution within Clone Libraries of Ethanol Stimulated Chamber Core Sediment**

| | clone library (%) | | |
|---|---|---|---|
| phyla | core 1 | core 2 | core 3 |
| $\beta$-Proteobacteria | 86 | 64 | 13 |
| $\gamma$-Proteobacteria | 6 | 21 | - |
| $\alpha$-Proteobacteria | 8 | 4 | 27 |
| Bacteroidetes | - | 3 | 29 |
| Firmicutes | - | 3 | 9 |
| Actinobacteria | - | 1 | 13 |
| Acidobacteria | - | 4 | 4 |
| $\delta$-Proteobacteria | - | - | 5 |
| Distribution | | | |
| no. taxa | 51 | 73 | 55 |
| no. OTUs | 7 | 16 | 14 |

which is capable of using ethanol for growth but does not reduce nitrate.

## Discussion

The constructed sediment pack composed of crushed Maynardsville Limestone and site sediment effectively increased influent pH from 4.7 to 6.9, with a corresponding 94% decrease in U concentrations in port 1 porewater. In a separate study, U concentrations decreased by 90% when acidic FRC groundwater was titrated to pH ~ 5 with sodium carbonate, although 70% of U reappeared in solution following additional titration (*17*). Energy dispersive X-ray analysis showed this initial decrease was due to U sorption or coprecipitation with Al- and Fe-hydroxides formed during titration and the authors attributed the subsequent increase to decreased zero points of charge of Al- and Fe-hydroxides or the formation of soluble U-carbonate complexes. In this study, Al concentrations in the acidic influent groundwater were decreased by 99% following pH adjustment (Supporting Information Figure 7). However, EXAFS spectral analysis detected the presence of uranyl orthophosphate $(UO_2)_3(PO_4)_2 \cdot 4H_2O_{(s)}$ in chamber core 1 sediment, which could control U solubility in this system (*60*). Using the average historical phosphate concentration in FW21 groundwater of 4.73 mg/L (data available online (*24*)), we estimate U(VI) solubility to be $1.29 \times 10^{-7}$ M, which just so happens to equal the current Maximum Contaminant Level (MCL) for U concentrations in drinking water (*61*) (see Supporting Information for calculations). Other U-phosphate minerals, such as autunite $(Ca(UO_2)_2(PO_4)_2 \cdot 10H_2O)$ and saleeite $(Mg(UO_2)_2(PO_4)_2 \cdot 10H_2O)$, are known to control U solubility in natural deposits (*62*) and hydroxyapatite $(Ca_{10}(PO_4)_6(OH)_2)$ has also been shown to effectively remove U from solution, showing promise for application in permeable reactive barriers (*63, 64*). Inorganic phosphates produced as byproducts of microbial activity have also recently been shown to facilitate precipitation of U-phosphate minerals (*65*). Additional research is required to determine the long-term stability of the observed uranyl orthophosphate mineral and its utility in controlling U solubility at the FRC.

Interestingly, nitrate and Tc concentrations decreased concomitantly in the chamber and to a lesser extent in the control. These results were confirmed in a well-mixed laboratory batch experiment where Tc concentrations decreased during denitrification. Nitrate and Tc were also observed to decrease concomitantly and prior to iron reduction during in situ push−pull test conducted at the FRC (*16*). However, other sediment incubation (*66, 67*) and pure culture studies (*6, 67*) have shown that denitrification must be complete prior to Tc removal. Using the nitrate and nitrite concentrations measured in the batch system, we calculated a redox potential of 459 mV, which is much higher than the 38 mV required for thermodynamically favorable Tc reduction at pH 7 (calculations in Supporting Information). The mechanism of observed Tc removal in the chamber and control is unknown, although the apparent temperature dependence of Tc removal in the chamber suggests a biologically mediated mechanism.

Ethanol additions to acidic, high nitrate FRC groundwater sustained nitrate removal for 21 months and promoted growth of a largely denitrifying community. Community composition also varied spatially with distance along the chamber flow path in apparent response to shifts in porewater chemistry. The core 1 sediment 16S rRNA gene clone libraries were dominated by a single OTU (59% of sequences), which shared close homology with *Burkholderia fungorum*. *Burkholderia* species have been detected in acidic FRC sediments following ethanol additions (*19, 21*), in RNA-based clone libraries of pH-neutral FRC sediment that were not electron donor stimulated (*55*), and in iron-reducing enrichment cultures from pH-neutral FRC sediments (*68*). *Burkholderia* species are known to occupy diverse ecological niches, many of which are associated with nitrogen cycling and in particular denitrification (*69*−*72*). *Burkholderia cepacia* $PR1_{301}$ was shown to exhibit increased tolerance to nickel concentrations under acidic conditions (*73*), suggesting *Burkholderia* may have had a competitive advantage in core 1 sediment near the acidic influent groundwater in the chamber. The 16S rRNA gene clone library and Q-PCR analysis appeared to better capture core 1 sediment community composition as distinct DGGE bands were not observed for this sample. Groundwater pH was increased from 4.7 to 6.9 and nitrite concentrations were increased substantially in core 2 compared to core 1 (Table 1). *Burkholderia* were dominant in core 2 sediment as well (41%), although *Pseudomonas*, *Castellaniella*, and *Acidovorax* were also detected. *Castellaniella defragrans* (formerly *Alcaligenes defragrans* (*74*)) was previously identified as an important denitrifier in ethanol stimulated FRC sediments (*21*) and were also dominant in clone libraries constructed from hematite coupons incubated in acidic FRC groundwater (*75*). In another study, over half of all *nirS* genes detected in acidic FRC groundwater were highly similar to the *nirS* genes of *Alcaligenes faecalis* and *Pseudomonas stutzeri* (*76*), suggesting their potential importance in acidic FRC groundwater. *Castellaniella defragrans* and *Pseudomonas stutzeri* were detected in both clone libraries and DGGE analysis of core 2, confirming their presence in the chamber sediment under denitrifying conditions following pH adjustment. Groundwater pH was increased from 6.9 to 7.3, nitrate was decreased from 106 to 85 mM, and nitrite was increased from 5 to 8.5 mM in core 3. *Burkholderia* composed only 14% of sequences detected in core 3 and *Castellaniella* and *Pseudomonas* sequences were not detected. In contrast, DGGE band sequences from cores 3 and 4 and 29% of clone sequences detected in core 3 sediment shared close homology with an effluent treatment plant clone within the *Bacteroidetes* phylum (DQ531963, unpublished). The ecological role of this possibly fermentative bacterium is unclear.

Groundwater velocities at the FRC vary from 0.129 m $day^{-1}$ in the fractured saprolite (*26*) to 2 m $day^{-1}$ in the shallow, gravel-filled layer (Dave Watson, Pers. comm., 1998 tracer test Area 2). The average temperature of the FRC groundwater is 19.6 ± 2.8 °C (*24*). Based the range of FRC groundwater velocities and an approximated first-order denitrification rate obtained at ∼20 °C during the 14 month of the chamber experiment, we estimate that a denitrification biobarrier normal to groundwater flow would need to be at least 2.4−37 feet in length to provide adequate residence time for 99% nitrate removal (calculations in Supporting Information).

Multiple factors could contribute to poor in situ biobarrier performance and require additional consideration. For example, preferential flow path formation due to biomass accumulation (*77*) or solids deposition could ultimately reduce residence time within the treatment zone and decrease U and Tc removal efficiency. Precipitation of acid soluble metals with increased pH could encrust the limestone, thereby decreasing the rate of limestone dissolution and alkalinity production (*78*−*80*). These metal hydroxide precipitates could also fill pore space and decrease hydraulic conductivity. Indeed, ICP analysis of select chamber porewater samples ($n = 4$) confirmed that Al, Mn, and Ca concentrations in the acidic influent FRC groundwater were significantly decreased following pH adjustment (Supporting Information Figure 7). During the 21 months of the experiment, 2184 L of FRC groundwater were neutralized in the chamber, and this resulted in the deposition of an estimated 812 g of Ca, 400 g of Al, and 203 g of Mn in the chamber. Clearly solids deposition and associated decreases in hydraulic conductivity are important design considerations for in situ treatment of FRC groundwater. Long-term buffering capacity of the Maynardsville limestone for neutralizing the acidic FRC groundwater is also an important consideration.

Bioclogging (*77, 81*) or decreased water saturation during denitrification (*82*−*84*) and associated decreases in hydraulic conductivity are also important considerations for in situ biobarrier applications. In this study, hydraulic conductivity fluctuated with temperature and denitrification rates, suggesting a link between nitrogen gas production and decreased hydraulic conductivity. In a recent study, Istok et al. investigated the fate of nitrogen gas in a mixture of FRC saprolite and Maynardsville limestone analogous to the constructed sediment pack used in this study (*85*). Water containing 100 mM nitrate and 300 mM ethanol was repeatedly pulsed into a chamber and nitrate removal rates and gas saturation were monitored. Nitrogen bubbles were observed to coalesce and escape through connected pores and hydraulic conductivity did not decrease significantly during the experiment. In this study, gas bubbles were not visually observed because the chamber was covered with aluminum foil to prevent light infiltration and algal growth. Bubbling was observed at the chamber water table when all sediment cores were collected except for core 1 near the inlet where no bubbling was observed.

In our previous study we showed that ethanol additions to neutral pH, low nitrate FRC groundwater flowing through an above-ground constructed sediment pack stimulated denitrification, as well as iron and sulfate reduction and sustained U and Tc bioimmobilization for 20 months (*22*). The results of this study show that ethanol additions to acidic, high nitrate FRC groundwater flowing through an above-ground limestone sediment pack effectively increased pH and sustained nitrate removal for long time periods. Together these studies suggest that in situ bioimmobilization of U and Tc from nitric acid impacted FRC groundwater may be possible.

## Acknowledgments

This research was supported by Grants FG03-02ER63443, DE-FC02-96ER62278, and FG02-00ER62986 (subcontract FSU F48792) from the DOE Office of Science (OS), Office of Biological and Environmental Research (BER), Environmental Remediation Sciences Program (ERSP) (formerly Natural and Accelerated Bioremediation Research Program). Additional support was provided by Integrative Graduate Education and Research Traineeship (IGERT) grant from the National Science Foundation. The Advanced Photon Source (APS) is supported by the DOE OS, Office of Basic Energy Sciences under Contract DE-AC02-06CH11357. The Materials Research Collaborative Access Team (MR-CAT) operations are supported by the US DOE OS and the MR-CAT member institutions. The PNC/XOR facilities are supported by the US DOE OS, the APS, a major facilities access grant from NSERC, the University of Washington, and Simon Fraser University. We also thank Jesse Jones, Robert Laughman, Ben Garcia, Ellie Selko, Melora Park, and Mohammad Azizian for their help in field and laboratory work.

## Supporting Information Available

Supporting figures, tables, and calculations are available free of charge via the Internet at http://pubs.acs.org.

## Literature Cited

(1) Lovely, D. R.; Phillips, E. J. P.; Gorby, Y. A.; Landa, E. R. Microbial reduction of uranium. *Nature* **1991**, *350*, 413–416.

(2) Lovely, D. R.; Roden, E. E.; Phillips, E. J. P.; Woodward, J. C. Enzymatic iron and uranium reduction by sulfate-reducing bacteria. *Mar. Geol.* **1993**, *113*, 41–53.

(3) Tebo, B. M.; Obraztsova, A. Y. Sulfate-reducing bacterium grows with Cr(VI), U(VI), Mn(IV) and Fe(III) as electron acceptors. *FEMS Microbiol. Lett.* **1998**, *162*, 193–198.

(4) Suzuki, Y.; Kelly, S. D.; Kemner, K. M.; Banfield, J. F. Enzymatic U(VI) reduction by Desulfosporosinus species. *Radiochim. Acta* **2004**, *92*, 11–16.

(5) De Luca, G.; De Pascale, P.; Dermoun, Z.; Rousset, M.; Vermeglio, A. Reduction of Tc(VII) by *Desulfovibrio fructosovorans* Is Mediated by the Nickel-Iron Hydrogenase. *Appl. Environ. Microbiol.* **2001**, *67* (10), 4583–4587.

(6) Lloyd, J. R.; Cole, J. A.; Macaskie, L. E. Reduction and Removal of Heptavalent Technetium from Solution by *Escherichia coli*. *J. Bacteriol.* **1997**, *179* (6), 2014–2021.

(7) Lloyd, J. R.; Ridley, J.; Khizniak, T.; Lyalikova, N. N.; Macaskie, L. E. Reduction of Technetium by *Desulfovibrio desulfuricans*: Biocatalyst Characterization and Use in a Flowthrough Bioreactor. *Appl. Environ. Microbiol.* **1999**, *65*, 2691–2696.

(8) Lloyd, J. R.; Chesnes, J.; Glasauer, S.; Bunker, D. J.; Livens, F. R.; Lovely, D. R. Reduction of actinides and fission products by Fe(III)-reducing bacteria. *Geomicrobiol. J.* **2002**, *19*, 103–120.

(9) Lloyd, J. R.; Sole, V. A.; VanPraagh, C. V. G.; Lovley, D. R. Direct and Fe(II)-mediated reduction of technetium by Fe(III)-reducing bacteria. *Appl. Environ. Microbiol.* **2000**, *66* (9), 3743–3749.

(10) Fredrickson, J. K.; Kostandarithes, H. M.; Li, S. W.; Plymale, A. E.; Daly, M. J. Reduction of Fe(III), Cr(VI), U(VI), and Tc(VII) by *Deinococcus radiodurans* R1. *Appl. Environ. Microbiol.* **2000**, *66*, 2006–2011.

(11) Abdelouas, A.; Lutze, W.; Gong, W.; Nuttall, H. E.; Strietelmeier, B. A.; Travis, B. J. Biological reduction of uranium in groundwater and subsurface soil. *Sci. Total Environ.* **2000**, *250*, 21–35.

(12) Senko, J. M.; Mohamed, Y.; Dewers, T. A.; Krumholz, L. R. Role for Fe(III) minerals in nitrate-dependent microbial U(IV) oxidation. *Environ. Sci. Technol.* **2005**, *39* (8), 2529–2536.

(13) Senko, J. M.; Istok, J. D.; Suflita, J. M.; Krumholz, L. R. In-situ evidence for uranium immobilization and remobilization. *Environ. Sci. Technol.* **2002**, *36* (7), 1491–1496.

(14) Wan, J. M.; Tokunaga, T. K.; Brodie, E.; Wang, Z. M.; Zheng, Z. P.; Herman, D.; Hazen, T. C.; Firestone, M. K.; Sutton, S. R. Reoxidation of bioreduced uranium under reducing conditions. *Environ. Sci. Technol.* **2005**, *39* (16), 6162–6169.

(15) Sani, R. K.; Peyton, B. M.; Dohnalkova, A.; Amonette, J. E. Reoxidation of reduced uranium with iron(III) (hydr)oxides under sulfate-reducing conditions. *Environ. Sci. Technol.* **2005**, *39* (7), 2059–2066.

(16) Istok, J. D.; Senko, J. M.; Krumholz, L. R.; Watson, D.; Bogle, M. A.; Peacock, A.; Chang, Y. J.; White, D. C. In situ bioreduction of technetium and uranium in a nitrate-contaminated aquifer. *Environ. Sci. Technol.* **2004**, *38* (2), 468–475.

(17) Gu, B. H.; Brooks, S. C.; Roh, Y.; Jardine, P. M. Geochemical reactions and dynamics during titration of a contaminated groundwater with high uranium, aluminum, and calcium. *Geochim. Cosmochim. Acta* **2003**, *67* (15), 2749–2761.

(18) Peacock, A. D.; Chang, Y. J.; Istok, J. D.; Krumholz, L.; Geyer, R.; Kinsall, B.; Watson, D.; Sublette, K. L.; White, D. C. Utilization of Microbial Biofilms as Monitors of Bioremediation. *Microb. Ecol.* **2004**, *47* (3), 284–292.

(19) North, N. N.; Dollhopf, S. L.; Petrie, L.; Istok, J. D.; Balkwill, D. L.; Kostka, J. E. Change in bacterial community structure during in situ Biostimulation of subsurface sediment cocontaminated with uranium and nitrate. *Appl. Environ. Microbiol.* **2004**, *70* (8), 4911–4920.

(20) Lovely, D. R. Bioremediation of Organic and Metal Contaminants with Dissimilatory Metal Reduction. *J. Ind. Microbiol.* **1995**, *14*, 85–93.

(21) Spain, A. M.; Peacock, A. D.; Istok, J. D.; Elshahed, M. S.; Najar, F. Z.; Roe, B. A.; White, D. C.; Krumholz, L. R. Identification and isolation of a *Castellaniella* species important during biostimulation of an acidic nitrate- and uranium-contaminated aquifer. *Appl. Environ. Microbiol.* **2007**, *73* (15), 4892–4904.

(22) Michalsen, M. M.; Goodman, B. A.; Kelly, S. D.; Kemner, K. M.; McKinley, J. P.; Stucki, J. W.; Istok, J. D. Uranium and Technetium Bio-Immobilization in Intermediate-Scale Physical Models of an In Situ Bio-Barrier. *Environ. Sci. Technol.* **2006**, *40*, 7048–7053.

(23) Brooks, S. C. Waste Characteristics of the Former S-3 Ponds and Outline of Uranium Chemistry Relevant to NABIR Field Research Center Studies; ORNL/TM-2001/27; Oak Ridge National Laboratory, Oak Ridge, TN, 2001.

(24) Environmental Remediation Sciences Program: Oak Ridge Field Research Center Site Descriptions. Available online at http://public.ornl.gov/nabirfrc/sitenarrative.cfm (accessed April 6, 2008).

(25) Gu, B. H.; Wu, W. M.; Ginder-Vogel, M. A.; Yan, H.; Fields, M. W.; Zhou, J.; Fendorf, S.; Criddle, C. S.; Jardine, P. M. Bioreduction of uranium in a contaminated soil column. *Environ. Sci. Technol.* **2005**, *39* (13), 4841–4847.

(26) Jardine, P. M.; Sanford, W. E.; Gwo, J. P.; Reedy, O. C.; Hicks, D. S.; Riggs, J. S.; Baily, W. B. Quantifying diffusive mass transfer in fractured shale bedrock. *Water Resour. Res.* **1999**, *35* (7), 2015–2030.

(27) Toride, N. L., F. J.; van Genuchten, M. , The CXTFIT Code for Estimating Transport Parameters from Laboratory or Field Tracer Experiments. Version 2.1. In Agriculture, U. S. D. o., Ed. Agricultural Research Service, U.S. Salinity Laboratory: Riverside, CA, 1999.

(28) Elias, D. A.; Senko, J. M.; Krumholz, L. R. A procedure for quantitation of total oxidized uranium for bioremediation studies. *J. Microbiol. Methods* **2003**, *53* (3), 343–53.

(29) Zhou, P.; Gu, B. H. , Extraction of oxidized and reduced forms of uranium from contaminated soils: Effects of carbonate and pH. *Environ. Sci. Technol.* 2005, *39*, 4435−4440.

(30) Segre, C. U.; Leyarovska, N. E.; Chapman, L. D.; Lavender, W. M.; Plag, P. W.; King, A. S.; Kropf, A. J.; Bunker, B. A.; Kemner, K. M.; Dutta, P.; Druan, R. S.; Kaduk, J. The MRCAT insertion device beamline at the Advanced Photon Source. *Synchrotron Radiat. Instrum.: US Natl. Conf. 11th* **2000**, *CP521*, 419–422.

(31) Bligh, E. G.; Dyer, W. J. *A rapid method of total lipid extraction and purification.* **1959**, *37* (8), 911–917.

(32) White, D. C.; Ringelberg, D. B. , Signature lipid biomarker analysis. *In Techniques in Microbial Ecology*, R. S. Burlage, R.A., D, Stahl, G. Geesey, and G. Sayler, Ed.Oxford University Press: New York, 1998; pp255−272.

(33) Guckert, J. B.; Antworth, C. P.; Nichols, P. D.; White, D. C. Phospholipid, ester-linked fatty acid profiles as reproducible assays for changes in prokaryotic community structure of estuarine sediments. *FEMS Microbiol. Ecol.* **1985**, *31* (3), 147–158.

(34) Mayberry, W. R.; Lane, J. R. Sequential alkaline saponification/acid hydrolysis/esterification: A one-tube method with enhanced recovery of both cyclopropane and hydroxylated fatty acids. *J. Microbiol. Methods* **1993**, *18* (1), 21–32.

(35) Michalsen, M. M.; Peacock, A. D.; Spain, A. M.; Smithgall, A. N.; White, D. C.; Sanchez-Rosario, Y.; Krumholz, L. R.; Istok, J. D. Sediment Microbial Community Shifts Correlate with Geochemistry in Model Bio-Barrier for Uranium and Technetium Removal

from Groundwater. *Appl. Environ. Microbiol.* **2007**, *73* (18), 5885–5896.
(36) Suzuki, M. T.; Taylor, L. T.; DeLong, E. F. Quantitative Analysis of Small-Subunit rRNA Genes in Mixed Microbial Populations via 5′-Nuclease Assays. *Appl. Environ. Microbiol.* **2000**, *66* (11), 4605–4614.
(37) Stults, J. R.; Snoeyenbos-West, O.; Methe, B.; Lovely, D. R.; Chandler, D. P. Application of the 5′ Fluorogenic Exonuclease Assay (TaqMan) for Quantitative Ribosomal DNA and rRNA Analysis in Sediments. *Appl. Environ. Microbiol.* **2001**, *67* (6), 2781–2789.
(38) Gruntzig, V.; Nold, S. C.; Zhou, J.; Tiedje, J. M.; Pseudomonas stutzeri Nitrite Reductase Gene Abundance in Environmental Samples Measured by Real-Time, P. C. R. *Appl. Environ. Microbiol.* **2001**, *67* (2), 760–768.
(39) Henry, S.; Baudoin, E.; Lopez-Gutierrez, J. C.; Martin-Laurent, F.; Brauman, A.; Philippot, L.; Quantification of denitrifying bacteria in soils by nirK gene targeted real-time, P. C. R. *J. Microbiol. Methods* **2004**, *59*, 327–335.
(40) Muyzer, G.; de Waal, E. C.; Uitterlinden, A. G. Profiling of complex microbial populations by denaturing gradient gel electrophoresis analysis of polymerase chain reaction-amplified genes coding for 16S rRNA. *Appl. Environ. Microbiol.* **1993**, *59* (3), 695–700.
(41) Catalano, J. G.; Brown, G. E. J. Analysis of uranyl-bearing phases by EXAFS spectroscopy: Interferences, multiple scattering, accuracy of structural parameters, and spectral differences. *Am. Mineral.* **2004**, *89*, 1004–1021.
(42) Dowling, N. J.; Widdel, F.; White, D. C. Phospholipid ester-linked fatty acid biomarkers of acetate-oxidizing sulfate reducers and other sulfide forming bacteria. *J. Gen. Microbiol.* **1986**, *132*, 1815–1825.
(43) Dowling, N. J. E.; Nichols, P. D.; White, D. C. Phospholipid fatty acid and infra-red spectroscopic analysis of a sulphate-reducing consortium. *FEMS Microbiol. Lett.* **1988**, *53* (6), 325–333.
(44) Aligupalli, S.P., F.; Larrson, L. Systematic study of the 3-hydroxy fatty acid composition of mycobacteria. *J. Bacteriol.* **1994**, *176*, 2962–2969.
(45) Edlund, A. N., P. D.; Roffey, R.; White, D. C. Extractable and lipopolysaccharide fatty acid and hydroxy acid profiles from *Desulfovibrio* species. *J. Lipid Res.* **1985**, *26*, 982–988.
(46) Thomas, T. D.; Batt, R. D. Degradation of cell constituents by starved Streptococcus lactis in relation to survival. *J. Gen. Microbiol.* **1969**, *58* (3), 347–362.
(47) Guckert, J. B.; Hood, M. A.; White, D. C. Phospholipid ester-linked fatty acid profile changes during nutrient deprivation of Vibrio cholerae: increases in the trans/cis ratio and proportions of cyclopropyl fatty acids. *Appl. Environ. Microbiol.* **1986**, *52* (4), 794–801.
(48) Kieft, T. L. R., D. B.; White, D. C. Changes in Ester-Linked Phospholipid Fatty Acid Profiles of Subsurface Bacteria during Starvation and Desiccation in a Porous Medium. *Appl. Environ. Microbiol.* **1994**, *60* (9), 3292–3299.
(49) Heipieper, H. J.; de Bont, J. A. Adaptation of Pseudomonas putida S12 to ethanol and toluene at the level of fatty acid composition of membranes. *Appl. Environ. Microbiol.* **1994**, *60* (12), 4440–4444.
(50) Kaneda, T. Iso-and anteiso-fatty acids in bacteria: biosynthesis, function, and taxonomic significance. *Microbiol. Rev.* **1991**, *55* (2), 288–302.
(51) Weerkamp, A.; Heinen, W. Effect of Temperature on the Fatty Acid Composition of the Extreme Thermophiles, Bacillus caldolyticus and Bacillus caldotenax. *J. Bacteriol.* **1972**, *109* (1), 443–446.
(52) Rilfors, L.; Wieslander, A.; Stahl, S. Lipid and protein composition of membranes of Bacillus megaterium variants in the temperature range 5 to 70 degrees C. *J. Bacteriol.* **1978**, *135* (3), 1043–1052.
(53) Hedrick, D. B.; White, D. C. Microbial respiratory quinines in the environment. I. A sensitive liquid chromatographic method. *J. Microbiol. Methods* **1986**, *5*, 243–254.
(54) Fields, M. W.; Yan, T. F.; Rhee, S. K.; Carroll, S. L.; Jardine, P. M.; Watson, D. B.; Criddle, C. S.; Zhou, J. Z. Impacts on microbial communities and cultivable isolates from groundwater contaminated with high levels of nitric acid-uranium waste. *FEMS Microbiol. Ecol.* **2005**, *53* (3), 417–428.
(55) Akob, D. M.; Mills, H. J.; Kostka, J. E. Metabolically active microbial communities in uranium-contaminated subsurface sediments. *FEMS Microbiol. Ecol.* **2007**, *59*, 95–107.
(56) Nyman, J. L.; Marsh, T. L.; Ginder-Vogel, M. A.; Gentile, M.; Fendorf, S.; Criddle, C. Heterogeneous response to biostimulation for U(VI) reduction in replicated sediment microcosms. *Biodegradation* **2006**, *17* (4), 303–316.
(57) Akob, D. M.; Mills, H. J.; Gihring, T. M.; Kerkhof, L.; Stucki, J. W.; Anastacio, A. S.; Chin, K.; Kusel, K.; Palumbo, A. V.; Watson, D.; Kostka, J. E. Functional Diversity and Electron Donor Dependance of Microbial Populations Capable of U(VI) Reduction in Radionuclide-Contaminated Subsurface Sediments. *Appl. Environ. Microbiol.* **2008**, *74* (10), 3159–3170.
(58) Brodie, E. L.; DeSantis, T. Z.; Joyner, D. C.; Baek, S. M.; Larsen, J. T.; Andersen, G. L.; Hazen, T. C.; Richardson, P. M.; Herman, D. J.; Tokunaga, T. K.; Wan, J. M.; Firestone, M. K. Application of a High-Density Oligonucleotide Microarray Approach to Study Bacterial Population Dynamics During Uranium Reduction and Reoxidation. *Appl. Environ. Microbiol.* **2006**, *72* (9), 6288–6298.
(59) Kuhner, C. H.; Frank, C.; Grie*β*hammer, A.; Schmittroth, M.; Acker, G.; Go*β*ner, A.; Drake, H. L. *Sporomusa silvacetica* sp. nov., an Acetogenic Bacterium Isolated from Aggregated Forest Soil. *Int. J. Syst. Bacteriol.* **1997**, *47* (2), 352–358.
(60) Sandino, A.; Bruno, J. The solubility of $(UO_2)_3(PO_4)_2 \cdot 4H_2O_{(s)}$ and the formation of U(VI) phosphate complexes: Their influence in uranium speciation in natural waters. *Geochim. Cosmochim. Acta* **1992**, *56*, 4135–4145.
(61) Environmental Protection Agency. List of Drinking Water Contaminants and MCLs. Available online in the Radionuclide Section: http://www.epa.gov/safewater/contaminants/index.html.
(62) Murakami, T. Mechanisms of Long-Term U Transport under Oxidizing Conditions. *Mater. Res. Soc. Symp. Proc.* **2006**, *893* (JJ07), 04.104.09.
(63) Fuller, C. C.; Bargar, J. R.; Davis, J. A. Molecular-Scale Characterization of Uranium Sorption by Bone Apatite Materials for a Permeable Reactive Barrier Demonstration. *Environ. Sci. Technol.* **2003**, *37* (20), 4642–4649.
(64) Fuller, C. C.; Bargar, J. R.; Davis, J. A.; Piana, M. J. Mechanisms of Uranium Interactions with Hydroxyapatite: Implications for Groundwater Remediation. *Environ. Sci. Technol.* **2002**, *36*, 159–165.
(65) Beazley, M. J.; Martinez, R. J.; Sobecky, P. A.; Taillefert, M. Uranium biomineralization as a result of bacterial phosphatase activity. *Abstr. Pap., Am. Chem. Soc.* **2006**, 231.
(66) Abdelouas, A.; Lutze, W.; Gong, W.; Nuttall, H. E.; Strietelmeier, B. A.; Travis, B. J. Microbial reduction of Tc99 in organic matter-rich soils. *Sci. Total Environ.* **2005**, *336*, 255–268.
(67) Li, X. Z.; Krumholz, L. R. Influence of nitrate on microbial reduction of pertechnetate. *Environ. Sci. Technol.* **2008**, *42* (6), 1910–1915.
(68) Petrie, L.; North, N. N.; Dollhopf, S. L.; Balkwill, D. L.; Kostka, J. E. Enumeration and characterization of iron(III)-reducing microbial communities from acidic subsurface sediments contaminated with uranium(VI). *Appl. Environ. Microbiol.* **2003**, *69* (12), 7467–7479.
(69) Viallard, V.; Poirier, I.; Coumoyer, B.; Haurat, J.; Wiebkin, S.; Ophel-Keller, K.; Balandreau, J. *Burkholderia graminis* sp. nov., a rhizospheric *Burkholderia speciea*, and reassesment of *[Pseudomonas] phenazinium, [Pseudomonas] pyrrocinia* and *[Pseudomonas] glathei as Burkholderia. Int. J. Syst. Bacteriol.* **1998**, *48*, 549–563.
(70) Van Borm, S.; Buschinger, A.; Boomsma, J. J.; Billen, J. *Tetraponera* ants have gut symbionts related to nitrogen-fixing root-nodule bacteria. *Proc. R. Soc. Lond. B Biol. Sci.* **2002**, *269*, 2023–2027.
(71) Coenye, T.; Vandamme, P. Diversity and significance of *Burkholderia* species occupying diverse ecological niches. *Envion. Microbiol.* **2003**, *5* (9), 719–729.
(72) Coenye, T.; Laevens, S.; Willems, A.; Ohlen, M.; Hannant, W.; Govan, J. R. W.; Gillis, M.; Falsen, E.; Vandamme, P. Burkholderia fungorum sp. nov. and Burkholderia caledonica sp. nov., two new species isolated from the environment, animals and human clinical samples. *Int. J. Syst. Evol. Microbiol.* **2001**, *51* (3), 1099–1107.
(73) Van Nostrand, J. D.; Sowder, A. G.; Bertsch, P. M.; Morris, P. J. Effect of pH on the Toxicity of Nickel and Other Divalent Metals to *Burkholderia cepacia* $PR1_{301}$. *Environ. Toxicol. Chem.* **2005**, *24* (11), 2742–2750.
(74) Kampfer, P.; Denger, K.; Cook, A. M.; Lee, S. T.; Jackel, U.; Denner, E. B. M.; Busse, H. J. *Castellaniella g*en. nov., to accomodate the phylogenetic lineage of *Alcaligenes defragrans*, and proposal of *Castellaniella defragrans g*en. nov., comb. nov. and *Castellaniella denitrificansI* sp. nov. *Int. J. Syst. Evol. Microbiol.* **2006**, *56*, 815–819.
(75) Reardon, C. L.; Cummings, D. E.; Petzke, L. M.; Kinsall, B. L.; Watson, D. B.; Peyton, B. M.; Geesey, G. G. Composition and diversity of microbial communities recovered from surrogate minerals incubated in an acidic uranium-contaminated aquifer. *Appl. Environ. Microbiol.* **2004**, *70* (10), 6037–6046.

(76) Yan, T.; Fields, M. W.; Wu, L.; Zu, Y.; Tiedje, J. M.; Zhou, J. Molecular diversity and characterization of nitrite reductase gene fragments (nirK and nirS) from nitrate- and uranium-contaminated groundwater. *Envion. Microbiol.* **2003**, *5* (1), 13–24.
(77) Seki, K.; Thullner, M.; Hanada, J.; Miyazaki, T. Moderate Bioclogging Leading to Preferential Flow Paths in Biobarriers. *Ground Water Monit. Rem.* **2006**, *26* (3), 68–76.
(78) Hedin, R. S.; Watzlaf, G. R. The effects of anoxic limestone drains on mine water chemistry: U.S. Bureau of Mines Special Publication. , Vol. SP06A, 1994, pp 185−194.
(79) Robbins, E. I.; Cravotta, C. A. I.; Savela, C. E.; Nord, G. L. J. Hydrobiogeochemical interactions in "anoxic" limestone drains for neutralization of acidic mine drainage. *Fuel* **1999**, *78*, 259–270.
(80) Naftz, D. L.; Morrison, S. J.; Davis, J. A.; Fuller, C. C. *Handbook of Groundwater Remediation Using Permeable Reactive Barriers: Applications to Radionuclides, Trace Metals, and Nutrients*; Academic Press: San Diego, CA, 2002.
(81) Taylor, S. W.; Jaffee, P. R. Biofilm growth and the related change in the physical properties of a porous medium I. Experimental investigation. *Water Resourc. Res.* **1990**, *26* (9), 2153–2159.
(82) Soares, M. I. M.; Belkin, S.; Abeliovich, A. Biological groundwater denitrification: laboratory studies. *Water Sci. Technol.* **1988**, *20* (3), 189–195.
(83) Soares, M. I. M.; Belkin, S.; Abeliovich, A. Clogging of microbial denitrification sand columns: gas bubbles or biomass accumulation. *Zeitschrift fur Wasser und Abwassar Forschung* **1989**, *22*, 20–24.
(84) Soares, M. I. M.; Braester, S.; Belkin, S.; Abeliovich, A. Denitrification in laboratory sand columns: carbon regime, gas accumulation and hydraulic properties. *Water Resour. Res.* **1991**, *25* (3), 325–332.
(85) Istok, J. D.; Park, M. M.; Peacock, A. D.; Oostrom, M.; Wietsma, T. W. An experimental Investigation of the Fate of Nitrogen Gas Produced During Denitrification. *Ground Water* **2007**, *45* (4), 461–467.

ES8012485